frontiers | Frontiers in Pharmacology

TYPE Original Research
PUBLISHED 05 November 2024
DOI 10.3389/fphar.2024.1486563

OPEN ACCESS

EDITED BY
Hua Li,
Air Force Medical University, China

REVIEWED BY
Pabitra Bikash Pal,
University of Pittsburgh, United States
Shenshen Wu,
Capital Medical University, China
Lixiao Zhou,
Chongqing Medical University, China

*CORRESPONDENCE
Yuxia Ma,
mayuxia@hebmu.edu.cn

†These authors have contributed equally to this work

RECEIVED 26 August 2024
ACCEPTED 24 October 2024
PUBLISHED 05 November 2024

CITATION
Zhang Y, Wen R, Ren J, Zhang F, Pei H, Zuo J and Ma Y (2024) Exploring the mechanism of sesamin for the treatment of $PM_{2.5}$-induced cardiomyocyte damage based on transcriptomics, network pharmacology and experimental verification.
Front. Pharmacol. 15:1486563.
doi: 10.3389/fphar.2024.1486563

Exploring the mechanism of sesamin for the treatment of $PM_{2.5}$-induced cardiomyocyte damage based on transcriptomics, network pharmacology and experimental verification

Yadong Zhang†, Rui Wen†, Jingyi Ren†, Fan Zhang, Huanting Pei, Jinshi Zuo and Yuxia Ma*

Department of Nutrition and Food Hygiene, School of Public Health, Hebei Medical University, Hebei Key Laboratory of Environment and Human Health, Shijiazhuang, China

Introduction: Exposure to fine particulate matter ($PM_{2.5}$) is known to be associated with cardiovascular diseases. Sesamin (Ses) is a natural phenolic compound found in sesame seeds and sesame oil. Ferroptosis is a novel mode of cell death characterised by iron-dependent lipid peroxidation. This study aims to explore whether $PM_{2.5}$ can induce ferroptosis in H9C2 cells and to investigate the precise protective mechanism of Ses.

Methods: Based on transcriptomic data, $PM_{2.5}$ may induce ferroptosis in cardiomyocytes. The ferroptosis inducer erastin and ferroptosis inhibitor ferrostatin-1 (Fer-1) were used to illustrate the mechanisms involved in $PM_{2.5}$-induced H9C2 cell injury. Using network pharmacology, the pharmacological mechanism and potential therapy targets of Ses were explored for the treatment of $PM_{2.5}$-induced cardiomyocyte injury. H9C2 cells were cultured and pretreated with Fer-1 or different concentrations of Ses, and then cardiomyocyte injury model was established using erastin or $PM_{2.5}$. Indicators of oxidative responses, including total superoxide dismutase, reduced glutathione, glutathione peroxidase and malondialdehyde, were measured. The expression levels of ferroptosis-related proteins were determined through Western blot analysis.

Results: Results demonstrate that $PM_{2.5}$ induces ferroptosis in H9C2 cells and Ses exerts a protective effect by suppressing ACSL4-mediated ferroptosis.

Discussion: Overall, these findings elucidate a novel mechanism by which Ses ameliorates the detrimental effects of $PM_{2.5}$ on cardiomyocytes.

KEYWORDS

sesamin, $PM_{2.5}$, heart injury, ferroptosis, network pharmacology, transcriptomics, ACSL4

Introduction

Environmental pollution has gradually become an urgent problem that must be addressed with the development of science and the economy. Data from the World Health Organisation (WHO) revealed that a substantial proportion, reaching up to 92%, of the global population resides in regions where air pollution levels exceed established thresholds. Fine particulate matter ($PM_{2.5}$), a prominent constituent of atmospheric contaminants, has been associated with major adverse health effects. $PM_{2.5}$ refers to microscopic particulates with an aerodynamic diameter of less than 2.5 μm (Bright et al., 2023). The WHO indicates that approximately 4.2 million deaths are attributed to $PM_{2.5}$ exposure each year (Morishita et al., 2018). In China, approximately 1.2 million premature deaths were caused by high levels of $PM_{2.5}$ in 2010 (Xie et al., 2016). The persistent presence and widespread distribution of $PM_{2.5}$ have substantial implications for human health and the atmospheric environment (Gao et al., 2022). Growing evidence indicates that $PM_{2.5}$ leads to adverse effects on the cardiovascular and respiratory systems (Kim et al., 2022; Li et al., 2022). Huang et al. (2019) provide evidence that chronic exposure to relatively high concentrations of $PM_{2.5}$ is positively correlated with stroke and its major subtypes. Liang et al. (2021) found that exposure to specific concentrations of $PM_{2.5}$ in a monsoon climate region notably raised the risk of emergency room visits for patients with atrial fibrillation (AF). Additionally, abundant evidence shows a strong association between $PM_{2.5}$ and atherosclerosis (Woo et al., 2021; Kwok et al., 2023; Macchi et al., 2023). Therefore, understanding the mechanism by which $PM_{2.5}$ causes cardiomyocyte damage and developing effective prevention and treatment strategies are imperative.

Since the 1990s, the potential impact of particulate matter in eliciting health effects through oxidative reactions has been recognised. Extensive efforts have been made to clarify the mechanisms underlying $PM_{2.5}$-induced adverse health effects. With the deepening of research, many new mechanisms of PM-induced toxicity share a common trigger: PM-induced oxidative stress (Vilas-Boas et al., 2024). Oxidative stress is an underlying cause of severe illnesses due to the oxidant–antioxidant imbalance. Reactive oxygen species (ROS) and cellular oxidative stress are considered inducers of diseases (Villarreal et al., 2020; Xiao et al., 2020). Ferroptosis, a novel type of programmed cell death characterised by lipid peroxidation, relies on iron-mediated oxidative damage (Dong et al., 2023). Several studies have shown that ferroptosis is involved in CVDs. Suppression of ferroptosis has a beneficial effect on cardiovascular injuries by alleviating mitochondrial damage and endothelial injury (Wang et al., 2020; Cai et al., 2022; Luo et al., 2022). Based on these studies, inhibiting oxidative stress and ferroptosis may be an effective therapeutic strategy to reduce the risk of adverse health effects caused by air pollution.

Growing evidence indicates that the relationship between human health and air pollution is influenced by dietary intake. Previous studies have shown that some active constituents in plant extracts, such as procyanidin and resveratrol, can substantially alleviate $PM_{2.5}$-induced cardiovascular damage (Chen et al., 2022; Yin et al., 2023). However, these active constituents are difficult to obtain in sufficient doses directly from food and are often consumed in the form of dietary supplements. Ses, a natural lignin-like compound separated from sesame seeds and sesame oil, has attracted widespread attention due to its extensive biological functions, including antioxidant and anti-inflammatory activities (Dalibalta et al., 2020; Majdalawieh et al., 2022). A meta-analysis indicated that daily dietary supplementation of 20–200 mg of Ses (approximately 4–40 g sesame seeds) can produce major cardiovascular benefits (Sun et al., 2022). Given the relative ease of obtaining Ses from dietary sources compared to other active constituents, its potential health benefits for the cardiovascular system warrant more extensive and rigorous investigation. At present, research evidence on the protective effect of Ses on $PM_{2.5}$-induced cardiomyocyte injury is still lacking. This study aimed to elucidate the mechanism of $PM_{2.5}$-induced cardiomyocyte damage and further explore the protective effects and targets of Ses in a $PM_{2.5}$-induced cardiomyocyte injury model.

Materials and methods

Bioinformatic analysis

The GSE dataset (GSE211949) was downloaded from NCBI GEO DataSets (https://www.ncbi.nlm.nih.gov/geo/). This dataset, generated using the GPL24247 platform, includes gene expression profiles from three normal mouse cardiomyocyte cells and 3 mouse cardiomyocyte cells treated with $PM_{2.5}$ at a concentration of 100 μg/mL. Differentially expressed genes (DEGs) were identified using the R package DESeq2 (version 1.40.2). A $|\log_2 FoldChange| \geq 1.5$ and adjusted $p < 0.05$ were set as the screening criteria. Pearson correlation coefficients were calculated using the cor. test function in R (version 4.0.3). Principal component analysis (PCA) was conducted using the FactoMineR package. The volcano plot and heatmap were generated using the "ggplot2" and "pheatmap" packages in R, respectively. The "clusterProfiler" package in R was used to perform Kyoto Encyclopaedia of Genes and Genomes (KEGG) enrichment analysis on the DEGs. The significance of enrichment analysis results was determined by a p-value below 0.05.

Computational pharmacology prediction

The candidate targets of Ses were predicted using Swiss Target Prediction (http://swisstargetprediction.ch/), Bioinformatics Analysis Tool for Molecular mechanism of Traditional Chinese Medicine (BATMAN-TCM, http://bionet.ncpsb.org.cn/batman-tcm/) (Liu et al., 2016), TargetNet (http://targetnet.scbdd.com/calcnet/index/) and Traditional Chinese Medicine Systems Pharmacology (TCMSP, https://www.tcmsp-e.com/#/home). Targets from the four aforementioned databases were synthesised to remove duplicate values and obtain the Ses-related targets. After organising the data, the VennDiagram package (version 1.7.3) in R software was used to find the intersection between the DEGs and the Ses targets. Subsequently, KEGG enrichment analysis was performed for the genes at the intersection. PPI analysis was conducted using the STRING database (STRING v11.5, https://cn.string-db.org) (Szklarczyk et al., 2019), and PPI networks were analysed using Cytoscape (version 3.9.1). The cytoHubba plugin was

used to calculate clustering coefficient scores, which were ranked from high to low.

Molecular docking analysis

The 2D molecular structure of the ligand, Ses, was obtained from the PubChem database (https://pubchem.ncbi.nlm.nih.gov/), and the AlphaFold structure of ACSL4 (receptor) was retrieved from the UniProt database (https://www.uniprot.org/). The 2D structure of Ses was converted into a 3D configuration using ChemBio3D Ultra (version 21.0.0.28), and the MM2 force field was used to optimise energy. Hydrogen atoms and charges were added to the ligand and receptor files using AutoDock Tools (version 1.5.7), and the files were subsequently exported in PDBQT format. After processing the structures of Ses and ACSL4, molecular docking was performed using AutoDockVina (version 1.1.2) (Trott and Olson, 2010) and visualised with PyMOL software (version 2.5).

Materials and reagents

H9C2 cell lines were supplied by Solarbio Science & Technology Co., Ltd. (Beijing, China). The $PM_{2.5}$ was collected using a membrane collection method on the Hebei Medical University campus. Ses (HPLC>98%) was purchased from Shanghai Aladdin Biochemical Technology Co., Ltd., (Shanghai, China). DMEM high-glucose medium, foetal bovine serum (FBS) and pancreatic digestive fluid (containing EDTA) were obtained from ZETA LIFE Inc. (CA, United States). Dimethyl sulfoxide (DMSO) and the ROS kit were purchased from Shanghai Biyotime Bio-technology (Shanghai, China). RIPA lysate, phosphate buffer (PBS), Phenylmethanesulfonyl fluoride protease inhibitor, skim milk powder, ECL Western blotting Substrate (ELC Plus), Tris-Base, Tween-20 and Fe^{2+} kit were purchased from Solarbio Science (Beijing, China). Anti-ACSL4 antibody, anti-β-actin polyclonal antibody, anti-GPX4 antibody and anti-SLC7A11 antibody were purchased from ABclonal Biotech Co., Ltd. (Wuhan, China). MDA, SOD, LDH, GSH, GSH-Px and BCA kits were purchased from Nanjing Jiancheng Bioengineering Institute (Nanjing, China). The C11 $BODIPY^{581/591}$ and JC-1 fluorescence probes were purchased from MedChemExpress (Shanghai, China). The CCK-8 kit was obtained from ZETA LIFE Inc. (CA, United States).

Cell culture

H9C2 cells were cultured in DMEM high-glucose medium containing 10% FBS and 1% dual antibiotics (containing 100 U/mL penicillin and 100 mg/mL streptomycin) at 37°C in a 5% CO_2 incubator.

$PM_{2.5}$ collection and preparation

The collection and preparation of $PM_{2.5}$ sample were performed in accordance with our previous study (Zhang et al., 2021). Briefly, $PM_{2.5}$ samples were collected using an air sampler, and the collected $PM_{2.5}$ quartz fibre filters were sectioned into small fragments, suspended in PBS and sonicated for 30 min. After filtration through gauze, the $PM_{2.5}$ suspension was subjected to vacuum freeze-drying for 48 h to obtain $PM_{2.5}$ dry powder, which was then stored at −80°C. The detailed chemical components of $PM_{2.5}$ have also been reported in our previous study.

Cell viability assay

CCK-8 kits were used to assess cell viability in this study. The H9C2 cell line was plated in 96-well plates at a density of 5×10^3 cells per well and cultured in 10% FBS medium for 12 h. Cells were then treated with different concentrations of Ses or $PM_{2.5}$ for 24 h. The CCK-8 solution was added to the culture medium at a ratio of 1:10 in each well. Cells were incubated at 37°C in a 5% CO_2 atmosphere for an additional 1 h. After the treatment, absorbance was measured using an enzyme-labelling instrument at 450 nm.

Determination of MDA, GSH and Fe^{2+}

Multiple oxidative stress markers (MDA, SOD and GSH) and Fe^{2+} levels in H9C2 cells were measured using assay kits according to the manufacturer's instructions.

Lipid peroxidation assay

The H9C2 cell line was plated in 6-well plates at a density of 3×10^5 cells per well and cultured in 10% FBS medium for 12 h. Drug intervention was applied after 12 h of cultures. Lipid ROS levels and mitochondrial membrane potential were measured by flow cytometry to determine whether $PM_{2.5}$ induced ferroptosis in H9C2 cells.

Western blot

The expression levels of ferroptosis-related proteins, including GPX4, SLC7A11, ACSL4 and LPCAT3, were measured by Western blot. Total protein from H9C2 cells was extracted using RIPA buffer containing protease inhibitors. The supernatant from the H9C2 cells was collected and subsequently denatured by boiling in 5× loading buffer for 5 min. After denaturation, equal amounts of proteins from each sample were electrophoresed by 10%–12% SDS–PAGE and transferred to a PVDF membrane. The membrane was then blocked in 5% skim milk for 2 h. Primary antibodies were incubated overnight at 4°C. The membrane was washed three times with TTBS, each wash lasting 10 min. Subsequently, the membrane was incubated with the secondary antibody for 40 min at room temperature. Finally, protein bands were detected using enhanced chemiluminescence.

Statistical analysis

The study analysis was performed using SPSS and GraphPad Prism. Data are expressed as the means ± SEM. Multiple group comparisons were conducted using one-way analysis of variance (one-way ANOVA). Differences were considered statistically significant when p-values were less than 0.05 ($p < 0.05$).

10.3389/fphar.2024.1486563

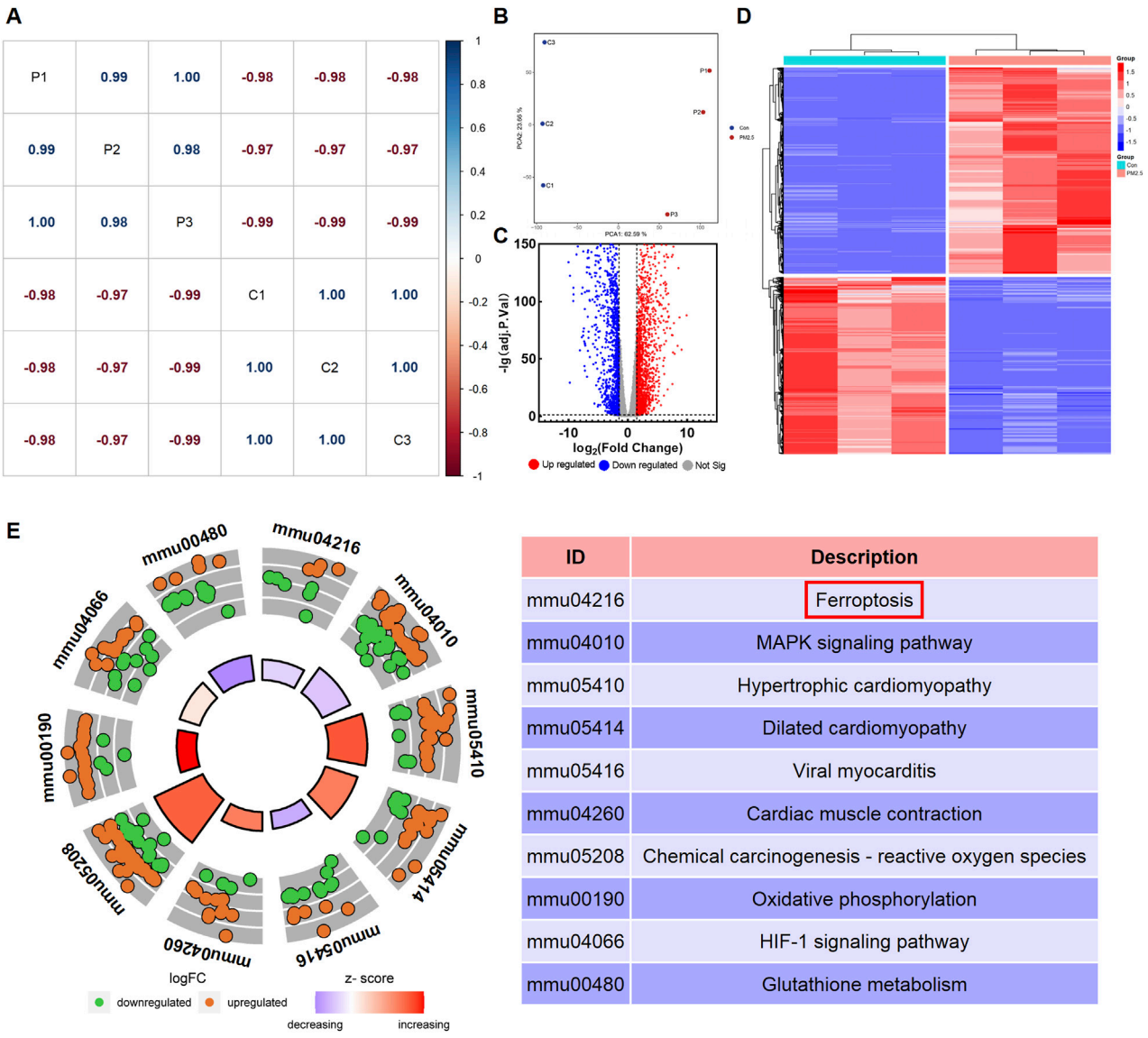

ID	Description
mmu04216	Ferroptosis
mmu04010	MAPK signaling pathway
mmu05410	Hypertrophic cardiomyopathy
mmu05414	Dilated cardiomyopathy
mmu05416	Viral myocarditis
mmu04260	Cardiac muscle contraction
mmu05208	Chemical carcinogenesis - reactive oxygen species
mmu00190	Oxidative phosphorylation
mmu04066	HIF-1 signaling pathway
mmu00480	Glutathione metabolism

FIGURE 1
$PM_{2.5}$ exposure altered the transcriptomics profile of HL-1 cell model. **(A)** Correlation analysis among sequencing samples. P represents $PM_{2.5}$-exposure group samples, and C represents control group samples. **(B)** Principal component analysis (PCA) between control group (Con) and $PM_{2.5}$-exposure group ($PM_{2.5}$). **(C)** Volcano plots of the differentially expressed genes (DEGs). **(D)** Heatmap of the DEGs. **(E)** Kegg enrichment analysis of the DEGs.

Results

$PM_{2.5}$ induces ferroptosis in cardiomyocyte cells at the transcriptional level

A correlation analysis was conducted to investigate the associations amongst different samples. A correlation coefficient close to one indicates a stronger positive correlation, whilst one close to −1 signifies a stronger negative correlation. Conversely, a correlation coefficient near 0 indicates a negligible or non-existent correlation between the two samples. The results indicate a strong positive correlation amongst samples within the same group and a strong negative correlation between samples from different groups (Figure 1A). The results of the unsupervised PCA demonstrated a distinct separation between the control group and the $PM_{2.5}$ exposure group samples. Principal component 1 (PC1) and principal component 2 (PC2) accounted for 62.59% and 23.66% of the total variance, respectively (Figure 1B). Differential expression analysis was performed using the 'DESeq2' R package to identify DEGs. The number of DEGs was illustrated using a volcano plot. A total of 3,212 DEGs were identified, meeting the threshold setting ($|\log_2 FoldChange| \geq 1.5$ and adjusted $p < 0.05$). Amongst these DEGs, 1729 genes were upregulated, and 1,483 genes were downregulated (Figure 1C). Subsequently, a heatmap of DEGs was presented in Figure 1D. Cluster analysis revealed the expression patterns of upregulated and downregulated genes across the samples. In the heatmap, red indicates upregulation, and blue indicates downregulation. KEGG enrichment analysis was used to

10.3389/fphar.2024.1486563

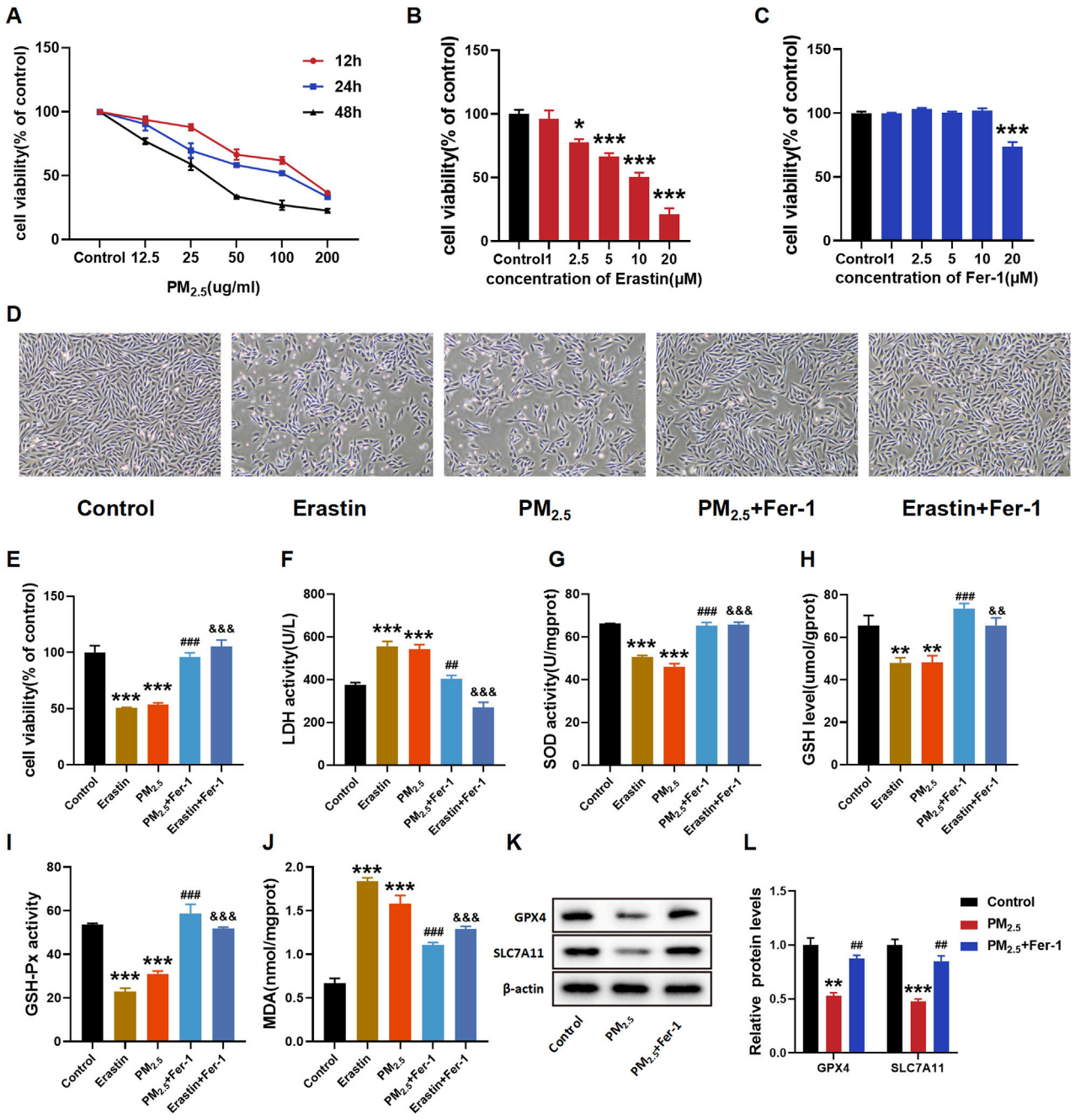

FIGURE 2
$PM_{2.5}$ exposure induced ferroptosis in H9C2 cells. **(A–C, E)** CCK8 was used to test the cell viability of each group of cells. **(D)** Morphology and growth of H9C2 cells under optical inverted microsope. **(F–J)** LDH, SOD, GSH, GSH-Px, MDA levels were analyzed by kits. **(K–L)** GPX4 and SLC7A11 levels were examined by Western blot. The data were expressed as mean ± SEM. All datas were obtained from three replicate experiments. $^{*}p < 0.05$, *versus* the Control. $^{**}p < 0.01$, *versus* the Control. $^{***}p < 0.001$, *versus* the Control. $^{\#\#}p < 0.01$, *versus* the $PM_{2.5}$ group. $^{\#\#\#}p < 0.001$, *versus* the $PM_{2.5}$ group. $^{\&\&}p < 0.01$, *versus* the Erastin group. $^{\&\&\&}p < 0.001$, *versus* the Erastin group.

determine the functions of DEGs. As illustrated in Figure 1E, the DEGs were primarily involved in ferroptosis, MAPK signalling pathway, hypertrophic cardiomyopathy, dilated cardiomyopathy, viral myocarditis, cardiac muscle contraction, chemical carcinogenesis-reactive oxygen species, oxidative phosphorylation, HIF-1 signalling pathway and glutathione metabolism. The detailed information of the DEGs involved in ferroptosis were shown in Supplementary Table S1.

$PM_{2.5}$ induces ferroptosis in H9C2 cells

H9C2 cells were treated with different concentrations of $PM_{2.5}$ for varying durations to determine the appropriate treatment time. Figure 2A shows a notable decrease in cell viability with increasing $PM_{2.5}$ concentration.

After exposure to $PM_{2.5}$, a decline in cell viability was observed, with the decrease being concentration-dependent. Notably, this

decline was more pronounced after 24 h of exposure compared to 12 and 48 h of exposure. The results indicated that the half inhibition concentration (IC50) of $PM_{2.5}$ was close to 100 μg/mL (Figure 2A). The IC 50 value of erastin and the optimal Fer-1 dose in H9C2 cells were then measured to determine the dose for subsequent experiments (Figures 2B,C, respectively). The H9C2 cell viability in Figure 2B exhibited a notable concentration-dependent decrease in response to erastin. In addition, at concentrations up to 10 μM, Fer-1 did not demonstrate remarkable cytotoxicity (Figure 2C). Cell morphology, cell viability and LDH release assays confirmed the damaging effects of $PM_{2.5}$ exposure, and Fer-1 can attenuate these changes (Figures 2D–F). Subsequently, the oxidative stress indices, including SOD, GSH, GSH-Px and MDA, were examined (Figures 2G–J). As expected, exposure to $PM_{2.5}$ remarkably decreased the levels of SOD, GSH and GSH-Px whilst increasing the level of MDA. However, Fer-1 substantially reversed these changes and alleviated oxidative stress. As two important biomarker proteins of ferroptosis, GPX4 and SLC7A11 exhibited relatively decreased expressions due to $PM_{2.5}$ exposure. In contrast, Fer-1 pretreatment remarkably increased the expressions of GPX4 and SLC7A11 (Figures 2K, L).

Pharmacological prediction of ses for mitigating cardiomyocyte cell injury induced by $PM_{2.5}$

A total of 16,360 targets of Ses were obtained from the Swiss Target Prediction, BATMAN-TCM, TargetNet and TCMSP databases, following the removal of partially overlapped targets. A total of 10 targets were obtained from Swiss Target Prediction, 16,359 targets from BATMAN-TCM, 4 targets from TargetNet and 17 targets from TCMSP (Figure 3A). According to Figure 3B, a total of 1859 targets were identified by integrating the Ses targets with the DEGs, namely, the targets of Ses involved in the treatment of $PM_{2.5}$-induced cardiomyocyte cells injury. Subsequently, KEGG enrichment analysis of the aforementioned intersection targets was conducted. The results showed that ferroptosis, chemical carcinogenesis-reactive oxygen species, glutathione metabolism, oxidative phosphorylation and cardiac muscle contraction were substantially enriched (Figure 3C). The PPI network was further constructed based on the genes enriched in ferroptosis and ranked by the clustering coefficient algorithm from high to low using the cytoHubba plugin (Figures 3D, E). The results revealed that ACSL4 had the highest score, followed by Slc39a14, Fth1, Cp, Hmox1, Tfrc, Prnp and Map1lc3a.

Ses attenuates ferroptosis caused by erastin in H9C2 cells

As shown in Figures 4A–D, after treatment with erastin, the cells shrank and lost their normal shape. However, pretreatment with Ses drastically inhibited this damage. H9C2 cells were treated with different concentrations of Ses (25–400 μM), and a CCK-8 assay was used to determine the viability of H9C2 cells. The results indicated no remarkable cytotoxicity of Ses at concentrations up to 100 μM (Figure 4E). Hence, concentrations of Ses, which include 25, 50 and 100 μM, were chosen as the intervention concentrations for subsequent experiments. An iCELLigence device was also used to monitor the cell index in real time (Figure 4F). The trend was consistent with the results of the CCK-8 assay. Based on the results of the CCK-8 assay and LDH release assays, Ses noticeably weakened the cellular damage caused by erastin (Figures 4G, H). Similarly, a decrease in the levels of GSH and an increase in the levels of MDA were observed after the administration of erastin. However, these alterations can be reversed by pretreatment with Ses (Figures 4I, J). The abovementioned results indicate that Ses is a potential candidate ferroptosis inhibitor and attenuates ferroptosis caused by erastin in H9C2 cells.

Ses attenuates cell injuries caused by $PM_{2.5}$ in H9C2 cells

Figures 5A–C illustrate the protective effect of different concentrations of Ses on cell morphology, cell viability and LDH release. A dose-dependent phylactic effect of Ses pretreatment was also observed.

Ses attenuates oxidative stress and mitochondrial damage caused by $PM_{2.5}$ in H9C2 cells

Concomitant with the progressive impairment of cardiomyocyte integrity, various markers of oxidative stress, such as SOD, GSH and GSH-Px, exhibited a notable decrease. However, with increased treatment levels of Ses, the levels of these crucial ROS scavengers were upregulated (Figures 6A, C, D). The MDA level, as the end product of lipid peroxidation, was downregulated after Ses administration (Figure 6B). The DCFH-DA staining (green) indicates an accumulation of ROS. The results revealed that Ses prevented ROS accumulation stimulated by $PM_{2.5}$ in H9C2 cells, and a dose-dependent therapeutic effect was notably observed (Figures 6E, F). In addition, the damage to mitochondrial membrane potential caused by $PM_{2.5}$ was remarkably reversed by Ses (Figures 6G, H). Collectively, these results indicate that Ses exerts strong antioxidant effects and inhibits mitochondrial damage in cardiomyocyte exposed to $PM_{2.5}$.

Ses attenuates ferroptosis caused by $PM_{2.5}$ in H9C2 cells

In ferroptosis, iron accumulation and lipid peroxidation are the two most important signs. Consequently, reducing the excess iron content is crucial for restraining ferroptosis. The present results indicate that $PM_{2.5}$ facilitates iron accumulation, whilst relatively high doses of Ses inhibit this progress (Figure 7A). The expression levels of ferroptosis-related proteins, including GPX4, SLC7A11, ACSL4 and LPCAT3, were measured to determine whether Ses inhibits cardiomyocyte ferroptosis. The results reveal that $PM_{2.5}$ downregulated the expression of GPX4 and SLC7A11 in H9C2 cells, whereas Ses restored the expression of both proteins (Figures 7B, C). Through molecular docking, the interaction between Ses and ACSL4 was confirmed (Figure 7D). The binding sites between Ses and ACSL4 were THR-159, ALA-182 and ARG-380. The binding energy was −9.1 kcal/mol (<−5 kcal/mol), indicating a strong binding affinity between the ligand

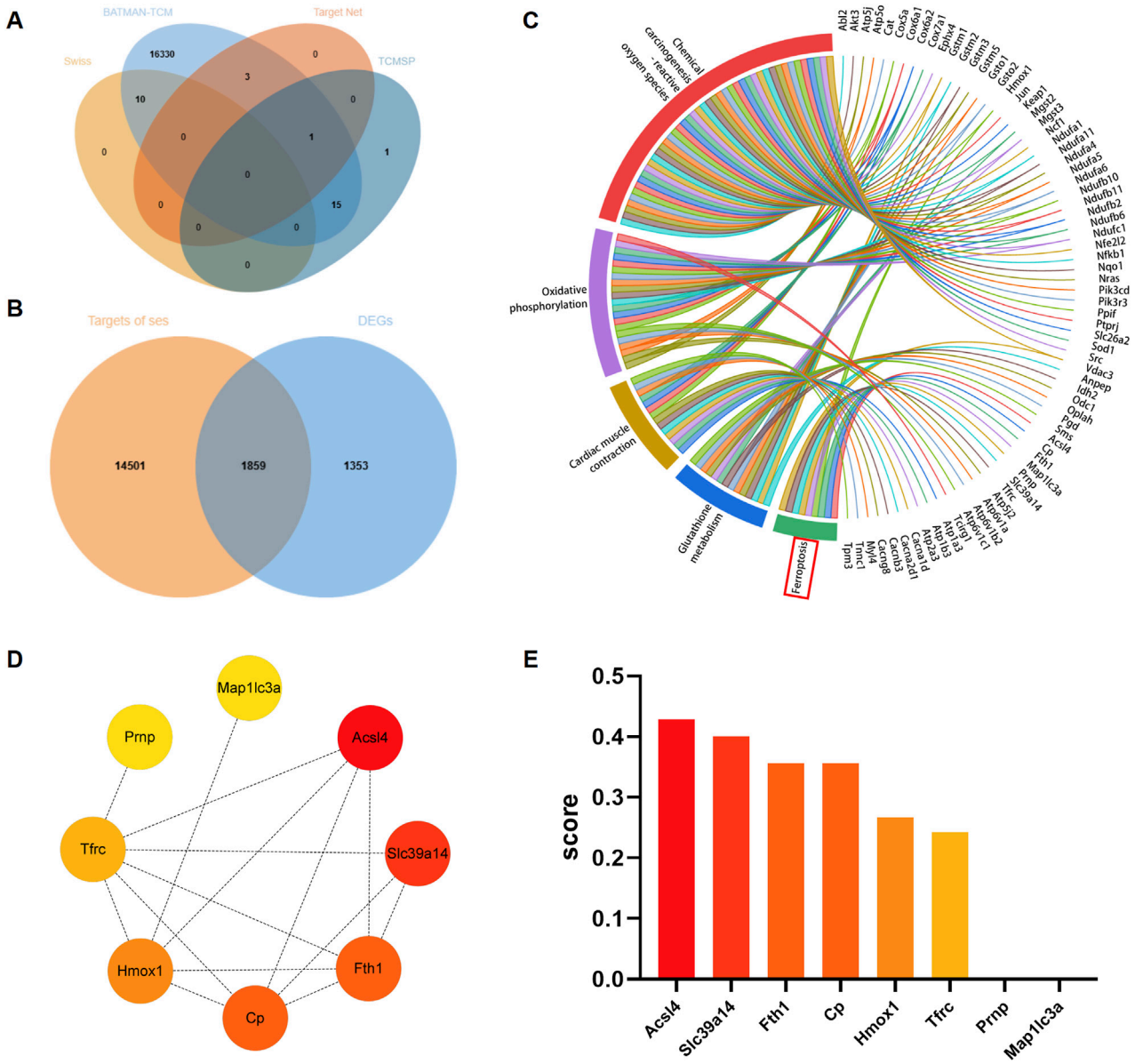

FIGURE 3
Analysis of core targets of sesamin (Ses) treatment for $PM_{2.5}$-induced ferroptosis in H9C2 cells based on network pharmacology. **(A)** Venn graph exhibiting the numbers of predicted Ses targets. **(B)** Venn diagram showing the interaction of Ses's targets and the differentially expressed genes (DEGs). **(C)** KEGG enrichment analysis of the interaction genes between Ses's targets and DEGs. **(D)** The enriched genes within the ferroptosis pathway were visualized through a protein-protein interaction network to identify hub genes. **(E)** The clustering coefficient scores of genes in the network were visualized via a histogram.

and the protein. Similarly, Ses downregulated the elevated levels of ACSL4 and LPCAT3 caused by $PM_{2.5}$ (Figures 7E, F). C11-BODIPY$^{581/591}$ is a fluorescent probe developed to detect lipid peroxidation. As shown in Figures 7G, H, the fluorescence signal intensity of the oxidised BODIPY remarkably increased after $PM_{2.5}$ exposure, whilst it was reduced by Ses pretreatment.

Discussion

The study provides evidence that Ses pretreatment exerts positive effects on $PM_{2.5}$-triggered cardiovascular injuries by inhibiting ferroptosis. A potential approach for the prevention of CVDs was identified. Clinical and epidemiological studies indicate that exposure to $PM_{2.5}$ increases the rate of cardiovascular death (Fiordelisi et al., 2017; Rajagopalan et al., 2018; Wang et al., 2019). However, scholarly investigations on the underlying mechanisms of CVDs due to exposure to $PM_{2.5}$ are rarely conducted. Several studies indicate a link between ferroptosis and CVDs. Ferroptosis plays a crucial role in doxorubicin- and ischemia/reperfusion-induced cardiomyopathy (Fang et al., 2019), myocardial infarction (Wang and Kang, 2021) and heart failure (Liu et al., 2018). The focus of this study was the role of ferroptosis in $PM_{2.5}$-triggered cardiovascular injuries. The results indicated that $PM_{2.5}$ exposure prominently

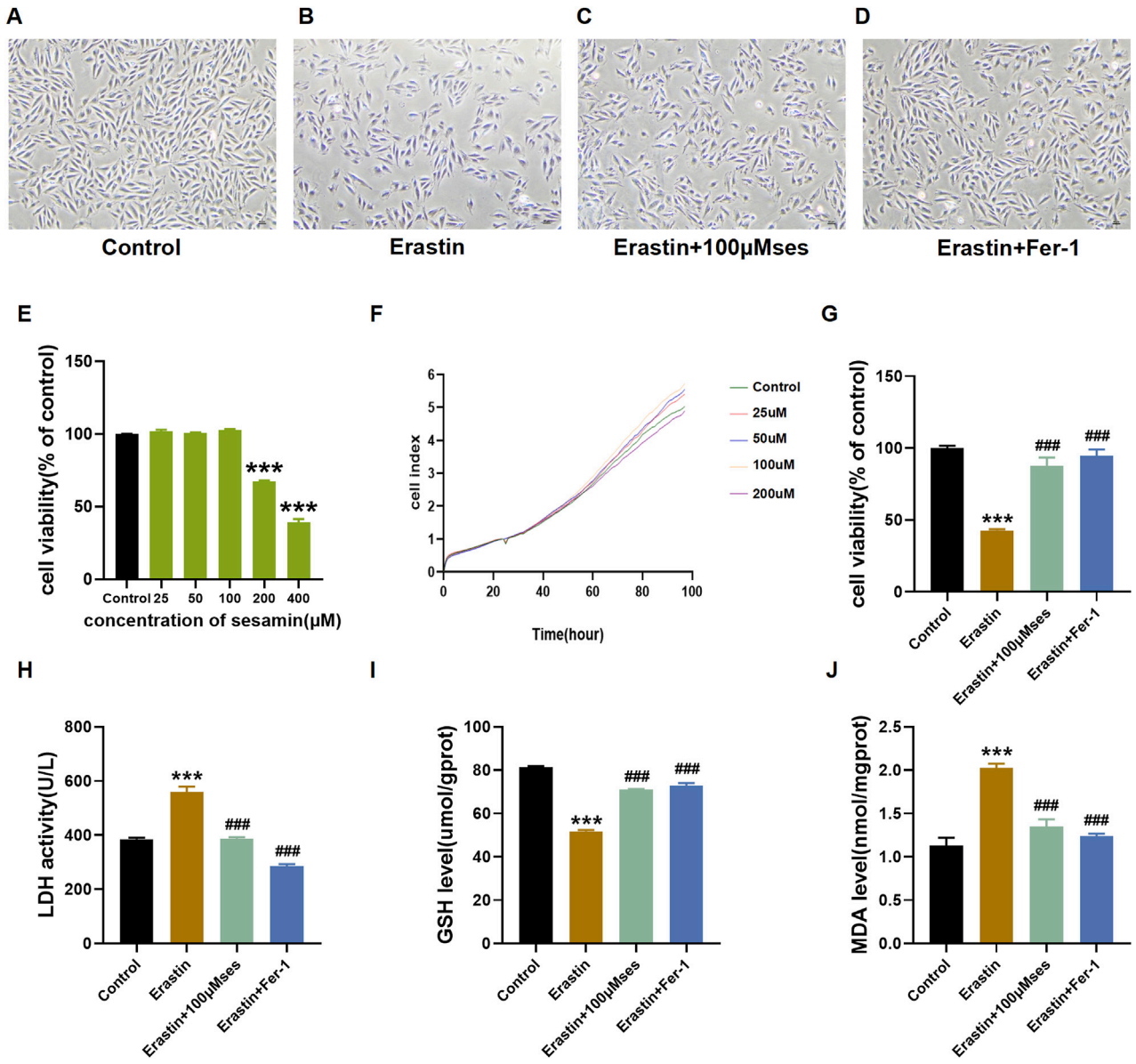

FIGURE 4
Ses attenuates ferroptosis caused by erastin **(A–D)** Morphology and growth of H9C2 cells under optical inverted microsope. **(E–G)** CCK8 and RTCA ICELLigence system were used to test the cell viability. **(H–J)** LDH, GSH, MDA levels were analyzed by kits. The data were expressed as mean ± SEM. All datas were obtained from three replicate experiments. ***$p < 0.001$, *versus* the Control. ###$p < 0.001$, *versus* the Erastin group.

increased the level of oxidative stress and caused disorders of iron metabolism. Ses pretreatment may mitigate these changes induced by $PM_{2.5}$. Consequently, Ses is considered beneficial for ferroptosis caused by $PM_{2.5}$.

Cardiovascular events caused by $PM_{2.5}$ may be indirectly attributable to the induction of oxidative stress (Kaihara et al., 2021). ROS plays a crucial role in oxidative stress (Li et al., 2021). In H9C2 cell experiments, previous studies have indicated that $PM_{2.5}$ (Cao et al., 2016) and erastin (Li et al., 2020) can increase levels of ROS. However, research on the toxicity similarity between erastin and $PM_{2.5}$ is still notably limited. In the present study, the morphology of H9C2 cells shifted clearly from fusiform to oblate in the erastin and $PM_{2.5}$ group. Fer-1 pretreatment improved cellular morphology, restoring a spindle-like shape and clear cytoplasm. The findings indicate that $PM_{2.5}$ has a detrimental impact on the activity of H9C2 cells, revealing that the ferroptosis inhibitor Fer-1 exhibited a repressive effect during this process. These results reveal that $PM_{2.5}$ may exert a negative, erastin-like effect. LDH is a marker of cellular damage. As a stable cytoplasmic enzyme existing in all cells, LDH is released into the cell culture supernatant when the plasma membrane is impaired (Kumar et al., 2018; Ma et al., 2021). In the current study, the level of LDH remarkably increased after $PM_{2.5}$ stimulation, and Fer-1 was able to attenuate this injury. $PM_{2.5}$ can elevate ROS levels through the multiple pathways, such as Fenton reaction or the activation of inflammatory cells. Excessive ROS generation modifies the expression of antioxidant enzymes, such as SOD, GSH and GSH-Px (Ragab et al., 2022). The levels of MDA reflect the degree of lipid peroxidation and cellular damage caused

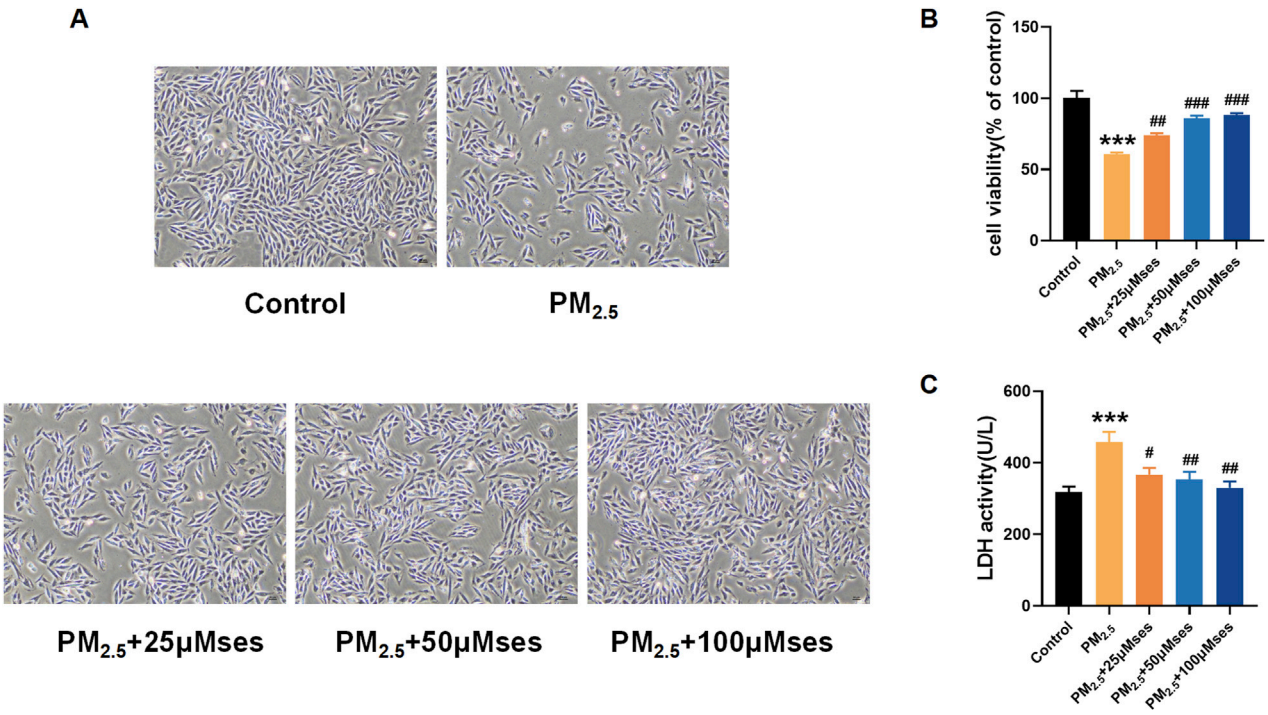

FIGURE 5
Ses moderates damages caused by $PM_{2.5}$ in H9C2 cells **(A)** Morphology and growth of H9C2 cells under optical inverted microsope. **(B)** CCK8 was used to test the cell viability of each group of cells. **(C)** LDH level was analyzed by kits. The data were expressed as mean ± SEM. All datas were obtained from three replicate experiments. ***$p < 0.001$, *versus* the Control. #$p < 0.05$, *versus* the $PM_{2.5}$ group. ##$p < 0.01$, *versus* the $PM_{2.5}$ group. ###$p < 0.001$, *versus* the $PM_{2.5}$ group.

by free radicals (Yang et al., 2021). In this study, the results showed that the activities of SOD, GSH and GSH-Px notably reduced in the $PM_{2.5}$ exposure group, and Fer-1 attenuated these changes. $PM_{2.5}$ exposure resulted in a remarkable increase in MDA content. However, Fer-1 diminished this change induced by $PM_{2.5}$. The above results indicate that the ferroptosis inhibitor Fer-1 can alleviate the damage caused by oxidative stress.

Ferroptosis was initially identified as a novel mechanism of cellular demise, characterised by unique attributes that differentiate it from other modes of cell death. This distinctive type of cell death is primarily induced by iron-dependent phospholipid peroxidation. Inhibition of GPX4 or System xc^- can potentially lead to the accumulation of lipid peroxides, thereby triggering the process of ferroptosis. System x_c^- is a transmembrane protein complex comprising two key subunits (SLC7A11 and SLC3A2). Cystine is transported from the extracellular space to the intracellular environment via System x_c^-. Once cystine is taken up into the cell, it is reduced to cysteine and utilised for the synthesis of GSH (Liu et al., 2022). Reduced (GSH) is converted to oxidised (GSSG) by GPX4 in the glutathione redox cycle (Shao et al., 2022). Previous research has shown that $PM_{2.5}$ entering cells can lead to elevated levels of Fe^{2+}, which may trigger the Fenton reaction. This reaction generates significant amounts of ROS, resulting in glutathione depletion, lipid peroxidation, and ultimately, ferroptosis (Guo et al., 2023). In our study, we also found that $PM_{2.5}$ exposure notably decreased the expression of SLC7A11 and GPX4, whilst Fer-1 pretreatment increased their expressions. The results of the study indicated that targeted inhibition of ferroptosis could be a viable approach for the prevention and treatment of CVDs.

Some phytochemicals, such as resveratrol, quercetin and anthocyanins, have been reported to reduce the damage of $PM_{2.5}$ on human health (Guo et al., 2024). However, most phytochemicals tend to have lower absorption rates in the human body due to their inherent properties, making them difficult to supplement directly through dietary intake. Ses, a lignan compound found in sesame seeds and oil, has been shown to have multiple health benefits. Previous studies have indicated that the absorption rate of Ses can exceed 90% (Umeda-Sawada et al., 1999), further emphasising its potential in improving human health. Li et al. found that taking Ses (50 and 100 mg) for 4 weeks can reduce mean pulmonary arterial pressure and right ventricular systolic pressure in monocrotaline-triggered hypertensive rats (Li et al., 2015). Loke et al. (Loke et al., 2010) also indicated that Ses can decrease the formation of atherosclerotic lesions. Despite the numerous therapeutic features of Ses, the persistence of the beneficial effects on $PM_{2.5}$-triggered cardiomyocyte injury remains unclear. This study initially demonstrated that Ses substantially attenuated cellular damage and oxidative stress triggered by erastin. Based on these results, the protective effect of different Ses concentrations on cardiovascular injury triggered by $PM_{2.5}$ was investigated. The results showed that Ses pretreatment remarkably reduced the levels of MDA and increased the activities of SOD, GSH and GSH-Px. The fluorescence intensity of ROS in the H9C2 cells subjected to $PM_{2.5}$ treatment exhibited a remarkably greater magnitude compared to the control group. Dose-dependent

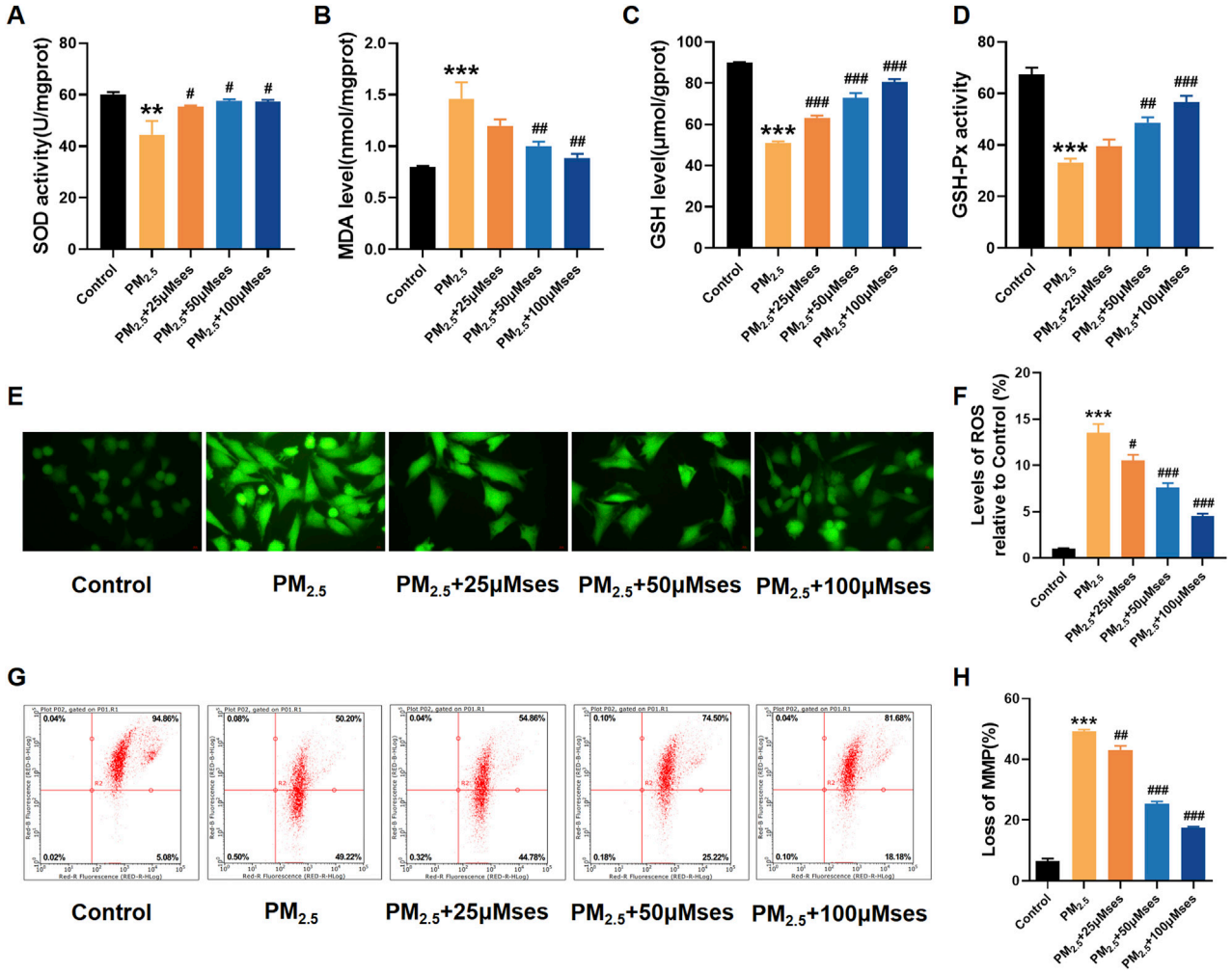

FIGURE 6
Ses weakens oxidative stress and mitochondrial damage caused by $PM_{2.5}$ in H9C2 cells. **(A–D)** SOD, MDA, GSH, GSH-Px levels were analyzed by kits. **(E)** The contents of ROS were measured by DCFH-DA. **(F)** Quantitative analyses of ROS. **(G)** Detection of MMP by flow cytometry JC-1 staining. **(H)** Quantitative analyses of JC-1. The data were expressed as mean ± SEM. All datas were obtained from three replicate experiments. $^{**}p < 0.01$, *versus* the Control. $^{***}p < 0.001$, *versus* the Control. $^{\#}p < 0.05$, *versus* the $PM_{2.5}$ group. $p < 0.01$, *versus* the $PM_{2.5}$ group. $^{\#\#\#}p < 0.001$, *versus* the $PM_{2.5}$ group.

differences were also observed in cells pretreated with different concentrations of Ses. The aforementioned results indicate that Ses pretreatment attenuates cellular damage and oxidative stress induced by $PM_{2.5}$. The effects of Ses on ferroptosis-related proteins GPX4 and SLC7A11 were further evaluated. The results indicated that the expressions of SLC7A11 and GPX4 markedly decreased in the $PM_{2.5}$ group, whilst Ses pretreatment restored their expression. These results reveal that Ses may act as a ferroptosis inhibitor to alleviate the toxicity of $PM_{2.5}$ in cardiomyocytes.

As a key lipid metabolism enzyme, the acyl-CoA synthetase long-chain family member 4 (ACSL4) plays a crucial role in ferroptosis (Ji et al., 2022). Lysophosphatidylcholine acyltransferase 3 (LPCAT3) is a crucial factor in producing lipoprotein (Xu et al., 2022). Polyunsaturated fatty acids (PUFAs) are the principal substrates of lipid peroxidation in the development of ferroptosis. ACSL4 and LPCAT3 accelerate ferroptosis through the integration of PUFAs into cellular phospholipids (Dixon et al., 2015; Yuan et al., 2016; Doll et al., 2017; Kagan et al., 2017). The network pharmacology results revealed that ACSL4 is the core target for Ses to exert protective effects, ranking first based on the clustering coefficient scores of genes. Therefore, ACSL4 may be a potential target for Ses to alleviate $PM_{2.5}$ cardiotoxicity. Western blot results indicated that the group of H9C2 cells treated with $PM_{2.5}$ exhibited elevated ACSL4 levels when compared to the control group. However, Ses treatment reversed these changes. Additionally, the findings are further validated through molecular docking analysis. Studies have shown that Protosappanin A can physically bind with ferroptosis-related protein ACSL4, inhibiting its phosphorylation and subsequent phospholipid peroxidation. While also preventing FTH1 autophagic degradation and subsequent release of ferrous ions (Fe^{2+}) (Cui et al., 2024). This may also be a possible mechanism by which Ses exerts its anti-ferroptotic activity.

Overall, Ses was found to attenuate $PM_{2.5}$-triggered cardiomyocyte injury. The potential mechanisms of Ses supplementation to mitigate $PM_{2.5}$-induced cardiomyocyte damage through the targeting of ACSL4-mediated ferroptosis. Hence, pursuing nutritional interventions that target ACSL4-

10.3389/fphar.2024.1486563

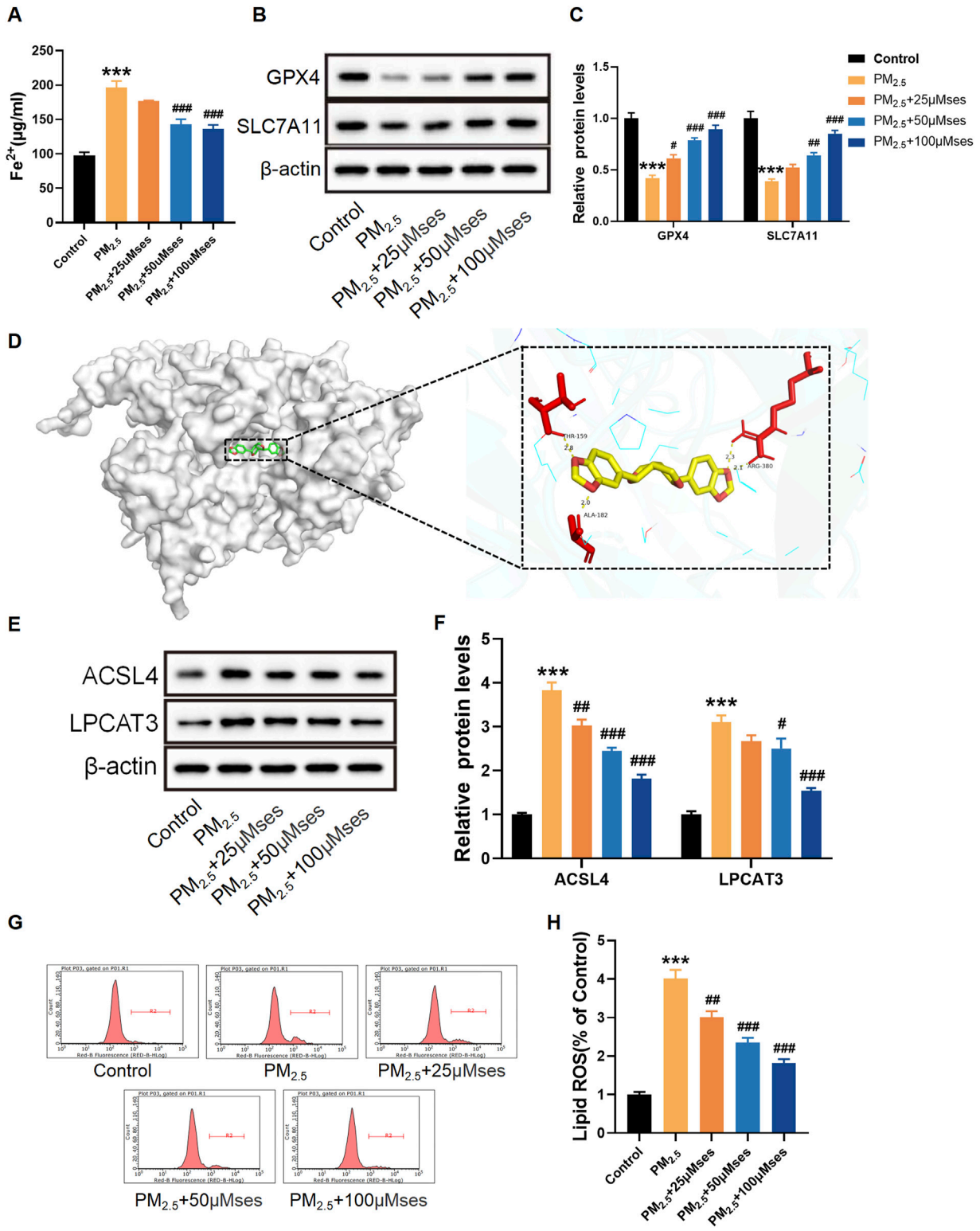

FIGURE 7
Sesamin (Ses) attenuates ferroptosis caused by $PM_{2.5}$ in H9C2 cells. **(A)** Quantitative analyses of Fe^{2+}. **(B)** GPX4 and SLC7A11 levels were examined by Western blot. **(C)** Quantitative analyses of GPX4 and SLC7A11. **(D)** Binding modes of Ses to ACSL4. **(E)** ACSL4 and LPCAT3 levels were examined by Western blot. **(F)** Quantitative analyses of ACSL4 and LPCAT3. **(G)** Lipid ROS with C11-BODIPY$^{581/591}$ was measured by Flow cytometry. **(H)** Quantitative analyses of lipid ROS. The data were expressed as mean ± SEM. All datas were obtained from three replicate experiments. ***$p < 0.001$, *versus* the Control. *$p < 0.05$, *versus* the $PM_{2.5}$ group. $^{\#\#}p < 0.01$, *versus* the PM2.5 group. $^{\#\#\#}p < 0.001$, *versus* the $PM_{2.5}$ group.

mediated ferroptosis presents a promising approach for developing effective countermeasures against $PM_{2.5}$-induced cardiomyocyte injury.

Data availability statement

Publicly available datasets were analyzed in this study. This data can be found here: https://www.ncbi.nlm.nih.gov/geo/query/acc.cgi?acc=GSE211949; (GSE211949).

Ethics statement

Ethical approval was not required for the studies on animals in accordance with the local legislation and institutional requirements because only commercially available established cell lines were used.

Author contributions

YaZ: Writing–original draft, Methodology, Conceptualization. RW: Writing–review and editing, Methodology. JR: Writing–review and editing, Conceptualization. FZ: Writing–review and editing, Methodology. HP: Writing–review and editing, Methodology. JZ: Writing–review and editing, Data curation. YM: Writing–review and editing, Funding acquisition.

Funding

The author(s) declare that financial support was received for the research, authorship, and/or publication of this article. This study was financially supported by the National Natural Science Foundation of China (No. 8237120896) and Undergraduate Innovation Experiment Project from Hebei Medical University (USIP2022047).

Acknowledgments

We thank all the authors for their contributions.

Conflict of interest

The authors declare that the research was conducted in the absence of any commercial or financial relationships that could be construed as a potential conflict of interest.

Publisher's note

Supplementary material

The Supplementary Material for this article can be found online at: https://www.frontiersin.org/articles/10.3389/fphar.2024.1486563/full#supplementary-material

References

Bright, A., Li, F., Movahed, M., Shi, H., and Xue, B. (2023). Chronic exposure to low-molecular-weight polycyclic aromatic hydrocarbons promotes lipid accumulation and metabolic inflammation. *Biomolecules* 13, 196. doi:10.3390/biom13020196

Cai, C., Guo, Z., Chang, X., Li, Z., Wu, F., He, J., et al. (2022). Empagliflozin attenuates cardiac microvascular ischemia/reperfusion through activating the AMPKα1/ULK1/FUNDC1/mitophagy pathway. *Redox Biol.* 52, 102288. doi:10.1016/j.redox.2022.102288

Cao, J., Qin, G., Shi, R., Bai, F., Yang, G., Zhang, M., et al. (2016). Overproduction of reactive oxygen species and activation of MAPKs are involved in apoptosis induced by PM2.5 in rat cardiac H9c2 cells. *J. Appl. Toxicol. JAT* 36, 609–617. doi:10.1002/jat.3249

Chen, J., Zhang, M., Zou, H., Aniagu, S., Jiang, Y., and Chen, T. (2022). Synergistic protective effects of folic acid and resveratrol against fine particulate matter-induced heart malformations in zebrafish embryos. *Ecotoxicol. Environ. Saf.* 241, 113825. doi:10.1016/j.ecoenv.2022.113825

Cui, J., Chen, Y., Yang, Q., Zhao, P., Yang, M., Wang, X., et al. (2024). Protosappanin A protects DOX-induced myocardial injury and cardiac dysfunction by targeting ACSL4/FTH1 axis-dependent ferroptosis. *Adv. Sci. Weinh. Baden-Wurtt. Ger.* 11, e2310227. doi:10.1002/advs.202310227

Dalibalta, S., Majdalawieh, A. F., and Manjikian, H. (2020). Health benefits of sesamin on cardiovascular disease and its associated risk factors. *Saudi Pharm. J. SPJ Off. Publ. Saudi Pharm. Soc.* 28, 1276–1289. doi:10.1016/j.jsps.2020.08.018

Dixon, S. J., Winter, G. E., Musavi, L. S., Lee, E. D., Snijder, B., Rebsamen, M., et al. (2015). Human haploid cell genetics reveals roles for lipid metabolism genes in nonapoptotic cell death. *ACS Chem. Biol.* 10, 1604–1609. doi:10.1021/acschembio.5b00245

Doll, S., Proneth, B., Tyurina, Y. Y., Panzilius, E., Kobayashi, S., Ingold, I., et al. (2017). ACSL4 dictates ferroptosis sensitivity by shaping cellular lipid composition. *Nat. Chem. Biol.* 13, 91–98. doi:10.1038/nchembio.2239

Dong, W., Jin, Y., Shi, H., Zhang, X., Chen, J., Jia, H., et al. (2023). Using bioinformatics and systems biology methods to identify the mechanism of interaction between COVID-19 and nonalcoholic fatty liver disease. *Med. Baltim.* 102, e33912. doi:10.1097/MD.0000000000033912

Du, Y., Xu, X., Chu, M., Guo, Y., and Wang, J. (2016). Air particulate matter and cardiovascular disease: the epidemiological, biomedical and clinical evidence. *J. Thorac. Dis.* 8, E8-E19–E19. doi:10.3978/j.issn.2072-1439.2015.11.37

Fang, X., Wang, H., Han, D., Xie, E., Yang, X., Wei, J., et al. (2019). Ferroptosis as a target for protection against cardiomyopathy. *Proc. Natl. Acad. Sci. U. S. A.* 116, 2672–2680. doi:10.1073/pnas.1821022116

Fiordelisi, A., Piscitelli, P., Trimarco, B., Coscioni, E., Iaccarino, G., and Sorriento, D. (2017). The mechanisms of air pollution and particulate matter in cardiovascular diseases. *Heart fail. Rev.* 22, 337–347. doi:10.1007/s10741-017-9606-7

Gao, L., Qin, J.-X., Shi, J.-Q., Jiang, T., Wang, F., Xie, C., et al. (2022). Fine particulate matter exposure aggravates ischemic injury via NLRP3 inflammasome activation and pyroptosis. *CNS Neurosci. Ther.* 28, 1045–1058. doi:10.1111/cns.13837

Guo, C., Lyu, Y., Xia, S., Ren, X., Li, Z., Tian, F., et al. (2023). Organic extracts in PM2.5 are the major triggers to induce ferroptosis in SH-SY5Y cells. *Ecotoxicol. Environ. Saf.* 249, 114350. doi:10.1016/j.ecoenv.2022.114350

Guo, Y., Zhao, J., Ma, X., Cai, M., Chi, Y., Sun, C., et al. (2024). Phytochemical reduces toxicity of PM2.5: a review of research progress. *Nutr. Rev.* 82, 654–663. doi:10.1093/nutrit/nuad077

Huang, K., Liang, F., Yang, X., Liu, F., Li, J., Xiao, Q., et al. (2019). Long term exposure to ambient fine particulate matter and incidence of stroke: prospective cohort study from the China-PAR project. *BMJ* 367, l6720. doi:10.1136/bmj.l6720

Ji, Q., Fu, S., Zuo, H., Huang, Y., Chu, L., Zhu, Y., et al. (2022). ACSL4 is essential for radiation-induced intestinal injury by initiating ferroptosis. *Cell Death Discov.* 8, 332. doi:10.1038/s41420-022-01127-w

Kagan, V. E., Mao, G., Qu, F., Angeli, J. P. F., Doll, S., Croix, C. S., et al. (2017). Oxidized arachidonic and adrenic PEs navigate cells to ferroptosis. *Nat. Chem. Biol.* 13, 81–90. doi:10.1038/nchembio.2238

Kaihara, T., Yoneyama, K., Nakai, M., Higuma, T., Sumita, Y., Miyamoto, Y., et al. (2021). Association of PM(2.5) exposure with hospitalization for cardiovascular disease in elderly individuals in Japan. *Sci. Rep.* 11, 9897. doi:10.1038/s41598-021-89290-5

Kim, M. J., Kang, J. Y., Kim, J. M., Moon, J. H., Lee, H. L., Jeong, H. R., et al. (2022). Effect of ethyl acetate fraction from eucommia ulmoides leaves on PM(2.5)-induced inflammation and cognitive dysfunction. *Oxid. Med. Cell. Longev.* 2022, 7157444. doi:10.1155/2022/7157444

Kumar, P., Nagarajan, A., and Uchil, P. D. (2018). Analysis of cell viability by the lactate dehydrogenase assay. *Cold Spring Harb. Protoc.* 2018, pdb.prot095497. doi:10.1101/pdb.prot095497

Kwok, C. Y. T., Poon, Y. K. P., Chook, P., Guo, D. S., Lin, C. Q., Yin, Y. H., et al. (2023). A potential strategy for atherosclerosis prevention in modernizing China - hyperhomocysteinemia, MTHFR C677T polymorphism and air pollution (PM2.5) on atherogenesis in Chinese adults. *J. Nutr. Health Aging* 27, 134–141. doi:10.1007/s12603-023-1889-x

Li, F., Liu, J., Tang, S., Yan, J., Chen, H., Li, D., et al. (2021). Quercetin regulates inflammation, oxidative stress, apoptosis, and mitochondrial structure and function in H9C2 cells by promoting PVT1 expression. *Acta histochem.* 123, 151819. doi:10.1016/j.acthis.2021.151819

Li, W., Li, W., Leng, Y., Xiong, Y., and Xia, Z. (2020). Ferroptosis is involved in diabetes myocardial ischemia/reperfusion injury through endoplasmic reticulum stress. *DNA Cell Biol.* 39, 210–225. doi:10.1089/dna.2019.5097

Li, X., Gao, Y., Li, S., and Yang, J. (2015). Effect of sesamin on pulmonary vascular remodeling in rats with monocrotaline-induced pulmonary hypertension. *Zhongguo Zhong Yao Za Zhi Zhongguo Zhongyao Zazhi China J. Chin. Mater. Medica* 40, 1355–1361.

Li, X., Li, Y., Yu, B., Zhu, H., Zhou, Z., Yang, Y., et al. (2022). Health and economic impacts of ambient air pollution on hospital admissions for overall and specific cardiovascular diseases in Panzhihua, Southwestern China. *J. Glob. Health* 12, 11012. doi:10.7189/jogh.12.11012

Liang, B., He, X., Du, X., Liu, X., and Ma, C. (2021). Effect of air quality on the risk of emergency room visits in patients with atrial fibrillation. *Front. Cardiovasc. Med.* 8, 672745. doi:10.3389/fcvm.2021.672745

Liu, B., Zhao, C., Li, H., Chen, X., Ding, Y., and Xu, S. (2018). Puerarin protects against heart failure induced by pressure overload through mitigation of ferroptosis. *Biochem. Biophys. Res. Commun.* 497, 233–240. doi:10.1016/j.bbrc.2018.02.061

Liu, J., Kang, R., and Tang, D. (2022). Signaling pathways and defense mechanisms of ferroptosis. *FEBS J.* 289, 7038–7050. doi:10.1111/febs.16059

Liu, Z., Guo, F., Wang, Y., Li, C., Zhang, X., Li, H., et al. (2016). BATMAN-TCM: a bioinformatics analysis Tool for molecular mechANism of traditional Chinese medicine. *Sci. Rep.* 6, 21146. doi:10.1038/srep21146

Loke, W. M., Proudfoot, J. M., Hodgson, J. M., McKinley, A. J., Hime, N., Magat, M., et al. (2010). Specific dietary polyphenols attenuate atherosclerosis in apolipoprotein E-knockout mice by alleviating inflammation and endothelial dysfunction. *Arterioscler. Thromb. Vasc. Biol.* 30, 749–757. doi:10.1161/ATVBAHA.109.199687

Luo, Y., Apaijai, N., Liao, S., Maneechote, C., Chunchai, T., Arunsak, B., et al. (2022). Therapeutic potentials of cell death inhibitors in rats with cardiac ischaemia/reperfusion injury. *J. Cell. Mol. Med.* 26, 2462–2476. doi:10.1111/jcmm.17275

Ma, X., Zhang, Y., Guan, M., Zhang, W., Tian, H., Jiang, C., et al. (2021). Genotoxicity of chloroacetamide herbicides and their metabolites *in vitro* and *in vivo*. *Int. J. Mol. Med.* 47, 103. doi:10.3892/ijmm.2021.4936

Macchi, C., Sirtori, C. R., Corsini, A., Mannuccio Mannucci, P., and Ruscica, M. (2023). Pollution from fine particulate matter and atherosclerosis: a narrative review. *Environ. Int.* 175, 107923. doi:10.1016/j.envint.2023.107923

Majdalawieh, A. F., Yousef, S. M., Abu-Yousef, I. A., and Nasrallah, G. K. (2022). Immunomodulatory and anti-inflammatory effects of sesamin: mechanisms of action and future directions. *Crit. Rev. Food Sci. Nutr.* 62, 5081–5112. doi:10.1080/10408398.2021.1881438

Morishita, M., Adar, S. D., D'Souza, J., Ziemba, R. A., Bard, R. L., Spino, C., et al. (2018). Effect of portable air filtration systems on personal exposure to fine particulate matter and blood pressure among residents in a low-income senior facility: a randomized clinical trial. *JAMA Intern. Med.* 178, 1350–1357. doi:10.1001/jamainternmed.2018.3308

Ragab, T. I. M., Zoheir, K. M. A., Mohamed, N. A., El Gendy, A. E.-N. G., Abd-ElGawad, A. M., Abdelhameed, M. F., et al. (2022). Cytoprotective potentialities of carvacrol and its nanoemulsion against cisplatin-induced nephrotoxicity in rats: development of nano-encasulation form. *Heliyon* 8, e09198. doi:10.1016/j.heliyon.2022.e09198

Rajagopalan, S., Al-Kindi, S. G., and Brook, R. D. (2018). Air pollution and cardiovascular disease: JACC state-of-the-art review. *J. Am. Coll. Cardiol.* 72, 2054–2070. doi:10.1016/j.jacc.2018.07.099

Shao, C., Yu, Z., Luo, T., Zhou, B., Song, Q., Li, Z., et al. (2022). Chitosan-coated selenium nanoparticles attenuate PRRSV replication and ROS/JNK-Mediated apoptosis *in vitro*. *Int. J. Nanomedicine* 17, 3043–3054. doi:10.2147/IJN.S370585

Sun, Y., Ren, J., Zhu, S., Zhang, Z., Guo, Z., An, J., et al. (2022). The effects of sesamin supplementation on obesity, blood pressure, and lipid profile: a systematic review and meta-analysis of randomized controlled trials. *Front. Endocrinol.* 13, 842152. doi:10.3389/fendo.2022.842152

Szklarczyk, D., Gable, A. L., Lyon, D., Junge, A., Wyder, S., Huerta-Cepas, J., et al. (2019). STRING v11: protein-protein association networks with increased coverage, supporting functional discovery in genome-wide experimental datasets. *Nucleic Acids Res.* 47, D607-D613–D613. doi:10.1093/nar/gky1131

Trott, O., and Olson, A. J. (2010). AutoDock Vina: improving the speed and accuracy of docking with a new scoring function, efficient optimization, and multithreading. *J. Comput. Chem.* 31, 455–461. doi:10.1002/jcc.21334

Umeda-Sawada, R., Ogawa, M., and Igarashi, O. (1999). The metabolism and distribution of sesame lignans (sesamin and episesamin) in rats. *Lipids* 34, 633–637. doi:10.1007/s11745-999-0408-2

Vilas-Boas, V., Chatterjee, N., Carvalho, A., and Alfaro-Moreno, E. (2024). Particulate matter-induced oxidative stress - mechanistic insights and antioxidant approaches reported in *in vitro* studies. *Environ. Toxicol. Pharmacol.* 110, 104529. doi:10.1016/j.etap.2024.104529

Villarreal, C. F., Santos, D. S., Lauria, P. S. S., Gama, K. B., Espírito-Santo, R. F., Juiz, P. J. L., et al. (2020). Bergenin reduces experimental painful diabetic neuropathy by restoring redox and immune homeostasis in the nervous system. *Int. J. Mol. Sci.* 21, 4850. doi:10.3390/ijms21144850

Wang, H., Shen, X., Liu, J., Wu, C., Gao, J., Zhang, Z., et al. (2019). The effect of exposure time and concentration of airborne PM(2.5) on lung injury in mice: a transcriptome analysis. *Redox Biol.* 26, 101264. doi:10.1016/j.redox.2019.101264

Wang, S., Wang, F., Yang, L., Li, Q., Huang, Y., Cheng, Z., et al. (2020). Effects of coal-fired PM(2.5) on the expression levels of atherosclerosis-related proteins and the phosphorylation level of MAPK in ApoE(-/-) mice. *BMC Pharmacol. Toxicol.* 21, 34. doi:10.1186/s40360-020-00411-8

Wang, X.-D., and Kang, S. (2021). Ferroptosis in myocardial infarction: not a marker but a maker. *Open Biol.* 11, 200367. doi:10.1098/rsob.200367

Woo, K. S., Chook, P., Hu, Y. J., Lao, X. Q., Lin, C. Q., Lee, P., et al. (2021). The impact of particulate matter air pollution (PM2.5) on atherosclerosis in modernizing China: a report from the CATHAY study. *Int. J. Epidemiol.* 50, 578–588. doi:10.1093/ije/dyaa235

Xiao, L.-L., Zhang, F., Zhao, Y.-L., Zhang, L.-J., Xie, Z.-Y., Huang, K.-Z., et al. (2020). Using advanced oxidation protein products and ischaemia-modified albumin to monitor oxidative stress levels in patients with drug-induced liver injury. *Sci. Rep.* 10, 18128. doi:10.1038/s41598-020-75141-2

Xie, R., Sabel, C. E., Lu, X., Zhu, W., Kan, H., Nielsen, C. P., et al. (2016). Long-term trend and spatial pattern of PM(2.5) induced premature mortality in China. *Environ. Int.* 97, 180–186. doi:10.1016/j.envint.2016.09.003

Xu, M., Guo, Y.-Y., Li, D., Cen, X.-F., Qiu, H.-L., Ma, Y.-L., et al. (2022). Screening of lipid metabolism-related gene diagnostic signature for patients with dilated cardiomyopathy. *Front. Cardiovasc. Med.* 9, 853468. doi:10.3389/fcvm.2022.853468

Yang, J., Zhang, K. Y., Bai, S. P., Wang, J. P., Zeng, Q. F., Peng, H. W., et al. (2021). The impacts of egg storage time and maternal dietary vitamin E on the growth performance and antioxidant capacity of progeny chicks. *Poult. Sci.* 100, 101142. doi:10.1016/j.psj.2021.101142

Yin, B., Zhang, X., Ren, J., Chen, F., Liang, J., Zhang, H., et al. (2023). The protective effects of procyanidin supplementation on PM(2.5)-induced acute cardiac injury in rats. *Environ. Sci. Pollut. Res. Int.* 30, 10890–10900. doi:10.1007/s11356-022-22938-5

Yuan, H., Li, X., Zhang, X., Kang, R., and Tang, D. (2016). Identification of ACSL4 as a biomarker and contributor of ferroptosis. *Biochem. Biophys. Res. Commun.* 478, 1338–1343. doi:10.1016/j.bbrc.2016.08.124

Zhang, L.-M., Lv, S.-S., Fu, S.-R., Wang, J.-Q., Liang, L.-Y., Li, R.-Q., et al. (2021). Procyanidins inhibit fine particulate matter-induced vascular smooth muscle cells apoptosis via the activation of the Nrf2 signaling pathway. *Ecotoxicol. Environ. Saf.* 223, 112586. doi:10.1016/j.ecoenv.2021.112586